Desalination and Water Treatment
www.deswater.com
doi: 10.5004/dwt.2019.23986

161 (2019) 171–180
September

TiO_2/SGNs as photocatalyst for degradation of water pollutants

Qinghua Mao, Dan Liu, Guoling Li, Qiaoping Wang, Chanjuan Xue, Yunshan Bai*

Key Laboratory of Applied Surface and Colloid Chemistry, Ministry of Education, School of Chemistry and Chemical Engineering, Shaanxi Normal University, Xi'An, Shaanxi, 710119, China, Tel. +86 29 81530726; email: baiys@snnu.edu.cn (Y. Bai)

Received 11 September 2018; Accepted 18 February 2019

ABSTRACT

A novel photocatalyst, titanium dioxide/spherical graphene nodules (TiO_2/SGNs) composites were prepared successfully by hydrothermal synthesis. SGNs were synthetized by simple thermal pyrolysis of methane in a chemical vapor deposition (CVD) reactor over home-made MgO from dolomite. The structure of TiO_2/SGNs composites was investigated by scanning electron microscopy, X-ray powder diffraction, Fourier transform infrared (FT-IR) spectroscopy, X-ray photoelectron spectroscopy (XPS), Raman spectroscopy and diffuse reflectance spectroscopy. The results showed that an anatase type TiO_2 was obtained, and TiO_2 and SGNs were successfully combined. FT-IR and XPS results lend support to the proposed mechanism of formation of TiO_2/SGNs composites through the bonding between oxygen vacancy sites in TiO_2 (Ti–O–Ti bonds) and in-plane oxygen functional (epoxy) groups in SGNs possibly via Ti–O–C bonds. The photocatalytic activity on methylene blue (MB) degradation proved that TiO_2/SGNs composites were more effective under UV light than pure TiO_2, SGNs and dark reaction. Kinetic studies indicated that MB degradation followed Langmuir–Hinshelwood model better, the increase of the initial concentration of MB, the apparent reaction rate constant decreased. The results indicated that the TiO_2/SGNs composites could be employed as an efficient photocatalyst for the removal of textile dyes from effluents.

Keywords: Spherical graphene nodules; CVD; TiO_2/SGNs composites; Methylene blue; Photocatalysis; Kinetics

1. Introduction

With the rapid development of dyestuff industry, dyestuff effluents become the main water pollution source, which is difficult to degrade. It has the characteristics of high concentration, high chroma and many refractory substances. Hence, it becomes difficult for the conventional treatment technology to treat the resulting wastewater effectively [1]. However, dye molecules can be thoroughly oxidized by photo-oxidizing agents in photocatalytic system, so they have attracted wide attention from domestic and foreign scholars [2].

It has been proved that photocatalytic oxidation technology has a broad application prospective in the degradation of various organic pollutants [3,4]. As a common environmental friendly photocatalytic material, titanium dioxide (TiO_2) has become a research hot spot for its high visible light transmittance, high refractive index, small particle size and strong ability to degrade pollutants [5]. In addition, the photocatalytic reaction conditions of TiO_2 are mild; the organic pollutants can be degraded at room temperature and atmospheric pressure.

The photocatalytic reaction can only occur in the presence of a photocatalyst. TiO_2 is a typical *n*-type semiconductor, which consists of the highest occupied orbital valence band and the lowest empty orbital conduction band. The gap band is between the conduction band and valence band [6]. When light with energy greater than or equal to 3.2 eV irradiated to the surface of TiO_2, photogenerated electrons (e^-) transmit from valence band to conduction band, and photogenerated hole (h^+) is produced in valence band [7]. The process is reversible, the electron–hole pair is easily recombined and heat is emitted, which results in reduced photocatalytic efficiency [8].

* Corresponding author.

Several strategies have been attempted to tailor the band gap of TiO_2 and to reduce the electron–hole recombination, namely doping TiO_2 with metallic [9], non-metallic [10], rare earth elements [7] and mixing TiO_2 with other nanomaterials [8]. One particularly promising approach lies on the mixing with carbon material [11]: TiO_2/graphene (GN), TiO_2/carbon nanotubes or C+N–TiO_2/HNTs [12], TiO_2/fullerenes, as these composite materials have been found to present improved electronic and optical properties for photocatalysis, increased adsorption of the pollutants onto the nanoparticles surface and increased separation of charge carriers, which effectively inhibits recombination [13].

In recent years, with the further study of photocatalytic mechanism of TiO_2/GN composite materials, it is widely believed that graphene itself can act as an electron trapping agent. The photogenerated electron–hole recombination [14] was inhibited, as the same time, the electron mobility increased greatly. The large specific surface area of graphene can also increase the active sites of photocatalytic reaction. Due to the large number of π–π conjugated double bonds on the surface of graphene, and a large number of adsorbed organic molecules can be enriched on the graphene plane. This provides a feasible path for hydroxyl radicals and photogenerated holes to degrade pollutants [15]. According to the reference reported, lower band gaps for the TiO_2/GN nanocomposites ranging from 2.94 to 2.35 eV than that of TiO_2 (3.08 eV) could be obtained [13].

TiO_2/GN nanocomposites have been produced by solvothermal [16], hydro-thermal [17,18], self-assembly [19] and in-situ synthesis [20]. These nanocomposites have been assessed for the degradation of pollutants. Methylene blue (MB) is a typical heterocyclic dyestuff. Because its aromatic structure is not easily destroyed, conventional methods are difficult to deal with it thoroughly. However, MB can be thoroughly oxidized by strong photocatalytic oxidation to non-toxic and harmless small molecular substances such as H_2O and CO_2 in the photocatalytic system. Therefore, MB dye is often used to test the photocatalytic performance of photocatalytic agents.

In the present study, spheroidal, lamellar and porous spherical graphene nodules (SGNs) were fabricated facilely on home-made MgO substrate by chemical vapor deposition (CVD) method, with CH_4 as carbon source and Ar as carrier gas. Then the TiO_2/SGNs composites were prepared by the hydrothermal synthesis method. The composites TiO_2/SGNs were characterized by various physico-chemical techniques, such as scanning electron microscopy (SEM), X-ray powder diffraction (XRD), Raman spectroscopy, Fourier transform infrared (FT-IR) spectroscopy, X-ray photoelectron spectroscopy (XPS) and diffuse reflectance spectroscopy (DRS). The present work comprises experimental investigation of the photocatalytic activity of TiO_2/SGNs composites with different contents of graphene. These composites were used to degrade methylene blue (MB) under UV-light irradiation to evaluate its photocatalytic performance, repetitiveness and kinetics.

2. Experimental section

2.1. Materials

The home-made MgO (98%) was derived from dolomite by calcium and magnesium separation technology. Methane (99.99%, Xi'an Tenglong Chemical Co., Ltd.), argon (99.99%, Xi'an Tenglong Chem. Co., Ltd.), HCl, NaOH (AR), tetrabutyl titanate (CP), and MB (Ind) were purchased (Medicine Group Chemical Reagent Co. Ltd., China) and used directly without further purification.

2.2. Synthesis of TiO_2/SGNs composites

SGNs synthesis was carried out using CVD method with methane as the carbon precursor according to the reference reported [21,22]. The CVD setup (FURNACE 1,200°C, Tianjin Zhong Ring Experimental Electric Furnace Co., Ltd.) contains a horizontal tubular furnace and gas flow control unit. Typically, 2 g MgO as the catalyst was transferred to quartz substrate equipped in CVD system and purged in an argon gas at a flow rate of 0.5 L min^{-1} for 80 min at 950°C, then methane (flow rate 0.9 L min^{-1}) was introduced and decomposed for 30 min. After that, the furnace was cooled to room temperature under argon atmosphere. The obtained material was treated with 2 mol L^{-1} HCl to remove MgO. The precipitate was then filtered, washed with distilled water several times and dried at 60°C for 48 h in a vacuum oven.

The synthesis of the TiO_2/SGNs composites was based on a one-step hydrothermal method according to reference reported [17]. In short, the 5 g tetrabutyl titanate and appropriate amount of SGNs (depending on the wt.% of the composites required – namely 0%, 0.2%, 0.4%, 0.8%, 1%, 2% and 2.2%) were dispersed in a mixture of 100 mL of ethanol and ultrasonication for 30 min. After that, this suspension was placed in a Teflon lined autoclave, sealed and heated to 180°C for 10 h. The resulting composites were then washed with deionized water and freeze-dried to avoid the agglomeration of the particles.

2.3. Characterization of TiO_2/SGNs composites

The surface morphology and elemental composition of the samples were examined using a Quanta 200 SEM (FEI, Shanghai, China) operating at 20 kV. The phase structure was characterized using a D8 Advance X-ray diffraction unit (Bruker, Germany). Raman spectra were recorded at room temperature using an inVia Reflex Renishaw with λ (532 nm) in the range of 100–3,000 cm^{-1}. FT-IR spectra were obtained using an FT-IR spectrometer (Tensor 27, Bruker, Germany) with KBr pellets in the frequency range 4,000–400 cm^{-1}. XPS (AXIS ULTRA, Kratos Analytical Ltd., Japan) was recorded to verify the formation and the structure of SGNs and TiO_2. DRS (UV-Vis-NIR spectrophotometer, PerkinElmer Inc., America) was used to measure light absorption and band energy E_g of TiO_2/SGNs composites in the range of 200–800 nm. Semiconducting optical absorption of direct forbidden band energy E_d was calculated as Eq. (1) [23]; indirect forbidden band energy E_i was calculated as Eq. (2) [24].

$$A = \frac{c\left(h\upsilon - E_d\right)^{1/2}}{h\upsilon} \tag{1}$$

$$A = \frac{c\left(h\upsilon - E_i\right)^{2}}{h\upsilon} \tag{2}$$

$$\upsilon = \frac{c}{\lambda} \tag{3}$$

where c in Eq. (1) is the absorption constant, A is absorbance, h is Planck constant (6.626×10^{-34} J s), c in Eq. (3) is velocity of light (3×10^{-8} m s^{-1}).

2.4. Photocatalytic degradation of MB

The photocatalytic capacities of SGNs and TiO_2/SGNs composites were evaluated through the degradation of MB, under UV light. For this, 100 mg of the catalysts were added to 100 mL of solution and magnetically stirred in the dark for 30 min, to achieve the adsorption–desorption equilibrium. Afterward, the UV photocatalytic degradations were carried out using a homemade photoreactor equipped with 18 W ultraviolet lamp (WD-9403E), from Beijing Liuyi Biotechnology Co. Ltd. (Beijing, China), an excitation peak of 254 nm, placed above the solution with 1 cm, UV lamp exposure area was 8.7×10^{-3} m^2. Each experiment was done in parallel for three times, with the measured arithmetic average as the midpoint, a line segment drawn in the direction of the magnitude of the measured value, half of the length of the segment equal to uncertainty is error bar. The reaction rate and efficiency of the degradation were determined by monitoring the intensity of the main absorbance peaks of MB (664 nm), using a UV–Vis spectroscopy (UVT6, Beijing Purkinje General Instrument Co. Ltd., Beijing, China). The degradation rate was calculated by Eq. (4) [25]:

$$R\% = \frac{C_0 - C_t}{C_0} \times 100\% \quad (4)$$

where C_0 and C_t (mg L^{-1}) represent the initial concentration and the concentration after time t irradiation.

In order to evaluate the stability of the prepared TiO_2/SGNs composites, after photocatalytic reaction of 60 min under ultraviolet light, the catalyst was recovered and reused directly. At the same time, after the reaction system reached the adsorption equilibrium in dark, the catalyst was recovered directly, then the catalyst was adsorbed again after dry treatment, and the adsorption process was repeated for four times, the stability of the prepared TiO_2/SGNs composites was characterized by Raman spectra.

2.5. Kinetics study

100 mg of the different samples were added to 100 mL MB solution with various initial concentrations and magnetically stirred in the dark for 30 min, then the ultraviolet lamp was turned on for the photocatalytic reaction, six groups of parallel experiments were conducted of each factor for different periods of time (10–60 min).

The kinetics of MB degradation was evaluated by photocatalyst followed Langmuir–Hinshelwood model, expressed by Eq. (5) [26] as follows:

$$\ln\frac{C_0}{C_t} = kt \quad (5)$$

where C_0 and C_t represent the initial concentration and the concentration after time t irradiation, respectively, and k is the degradation rate constant.

3. Results and discussion

3.1. Effect of SGNs percentage in TiO_2/SGNs on degradation of MB

It can be seen from Fig. 1 that the degradation rate of chromaticity increases with the increase of SGNs percentage in TiO_2/SGNs, and when the percentage of SGNs was higher than 2%, the degradation rate was no longer increased. In the process of hydrothermal reaction, TiO_2 nanoparticles were formed by the hydrolysis reaction of tetrabutyl titanate. With the increase of SGNs percentage, the large specific surface area of graphene and conjugations between methylene blue molecules and the aromatic rings of SGNs sheets, which could lead to the higher adsorptivity. At the same time, SGNs doped TiO_2 inhibited the combination of electron–hole pairs [27] and improved photocatalytic activity. Therefore, the % of SGNs in the composites is 2%.

A SGNs with loosened nucleus and compacted shell in porous lamellar (ca. 200 μm) structure, derived from thermal pyrolysis of CH_4 in a CVD reactor over at 950°C for 30 min, was obtained (Figs. 2a and b). TiO_2 consisted of aggregated spherical particles, originating clusters of TiO_2 particles (Figs. 2c and d) [28]. Regarding the composite, prepared by hydrothermal and sonication, it is expected that, during the hydrothermal treatment, the TiO_2 nanoparticles completely adhere to their surfaces. The EDX spectrum of TiO_2/SGNs confirms the presence of Ti, C and O elements, which can all be addressed to the successful formation of TiO_2/SGNs composites.

XRD was performed to assess the crystalline properties of TiO_2/SGNs composites (Fig. 3). The diffraction peaks observed at 25.3°, 37.8°, 48.0°, 53.9°, 55.0°, 62.8°, 68.8°, 70.3°, 75.1° and 76.1°) correspond to the characteristic anatase TiO_2 crystal planes (JCPDS cards 21–1272) [29], formed by butyl titanate gel reaction during hydrothermal reaction. The characteristic peak of SGNs at $2\theta = 25.5°$ (002) was observed, the corresponding d-spacing (3.43 Å) showed the two-dimensional ordering of SGNs [30]. There is no typical SGNs peaks (23°–26°) observed in the composite [31], maybe

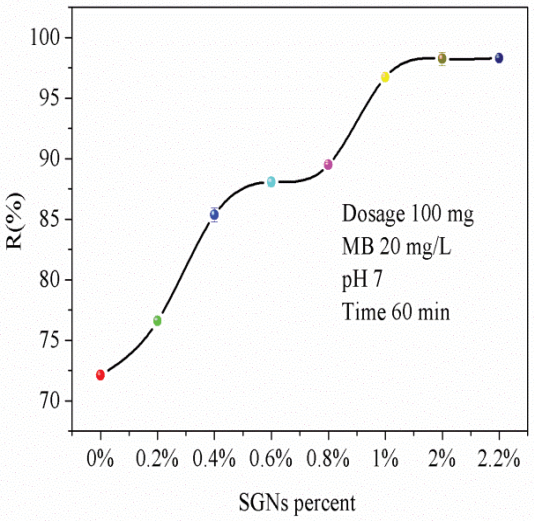

Fig. 1. Photocatalytic degradation of MB by TiO_2/SGNs with different SGNs percentage.

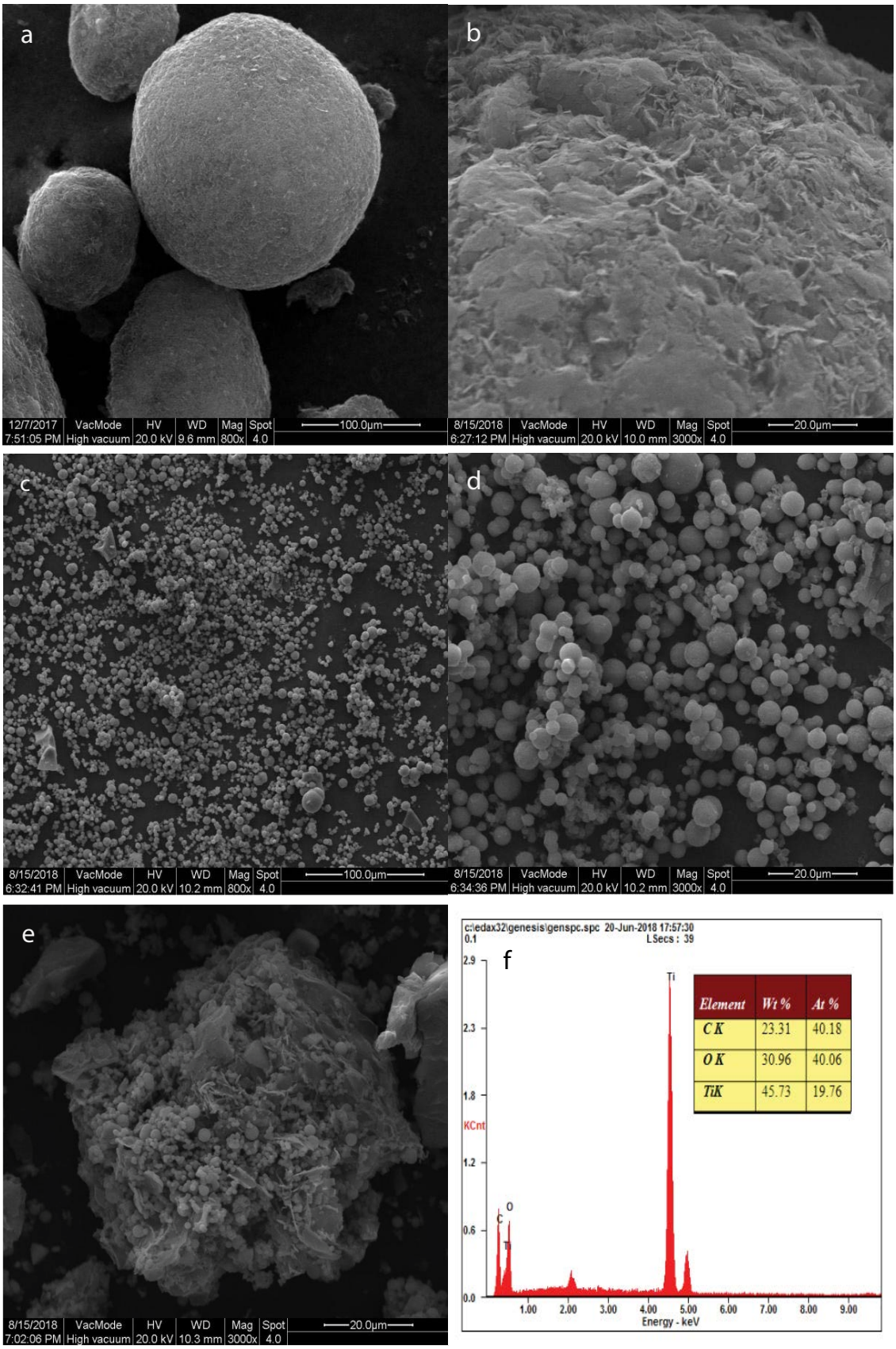

Fig. 2. SEM images of SGNs ((a) and (b)), TiO_2 ((c) and (d)) and TiO_2/SGNs composites (e) and its EDX (f).

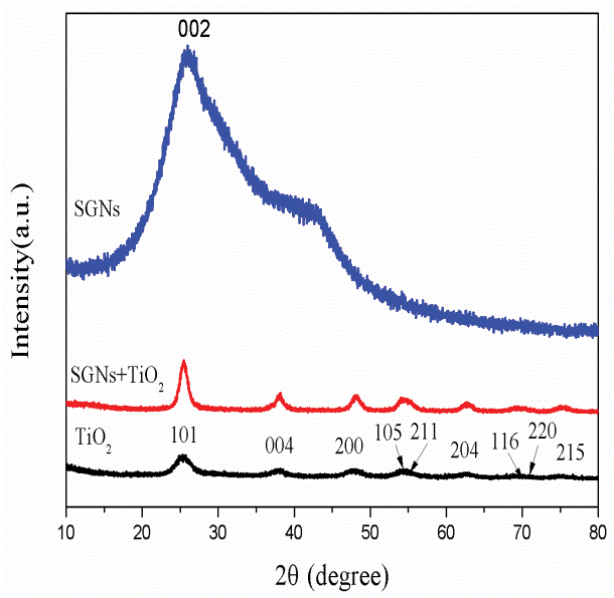

Fig. 3. XRD patterns of SGNs, TiO_2 and TiO_2/SGNs.

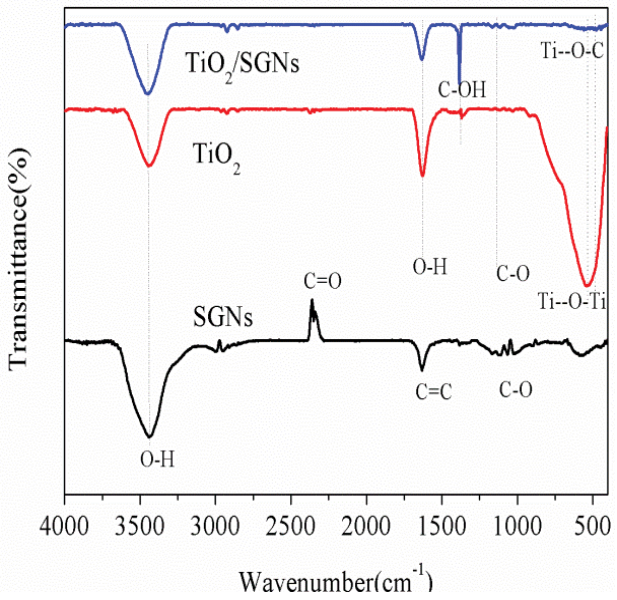

Fig. 4. FT-IR spectra of SGNs, TiO_2 and TiO_2/SGNs.

due to the lower percentage of SGNs in the composites, which overlap or screened by the (101) diffraction peak of TiO_2 [32].

In order to further confirm the crystalline quality and the formation of the chemical bonds in the TiO_2/SGNs composites, Raman spectrum was recorded in the range of 100–3,000 cm^{-1}. It showed that the characteristic absorption peaks of anatase type TiO_2 at E_{1g} = 148 cm^{-1}, B_{1g} = 393 cm^{-1}, $A_{1g} + B_{1g}$ = 513 cm^{-1}, E_{2g} = 635 cm^{-1}, which were consistent with the results of XRD [33]. The spectra reveal the presence of *D* (1.350 cm^{-1}) and *G* (1,580 cm^{-1}) due to breathing modes of sp^2 carbon atoms in rings and bond stretching between pairs of sp^2 carbon atoms, respectively, with an intensity ratio I_D/I_G of 1.21, which is directly related to the average size of the sp^2 carbon [34]. The *G* band is the result of first-order scattering of the E_{2g} mode observed for sp^2 carbon domains, and the 2*D* band is the most prominent feature of graphene [35]. The appearances of these bands confirm the formation of graphene structure and high degree of defect. The basic peak almost unchanged after photocatalytic degradation of MB, which indicated that the TiO_2/SGNs catalyst was stable.

FT-IR measurements were performed to assess the chemical interactions within the composites. The spectra obtained for the TiO_2, SGNs and TiO_2/SGNs samples are shown in Fig. 4. The broad band at around 3,433 cm^{-1} attributed to –OH stretching vibrations of physically adsorbed water molecules, and the absorption band at around 2,362 cm^{-1} attributed to C=O stretching vibrations of physically adsorbed carbon dioxide molecules. The absorption band at around 1,622 cm^{-1} corresponds to C=C stretching vibrations, suggesting the formation of SGNs with sp^2 hybrid. Additionally, for the TiO_2/SGNs composites, it is also possible to identify the peaks corresponding to hydroxyl C–OH (1,380 cm^{-1}) and epoxy C–O (1,122 cm^{-1}) stretching modes. Ti–O–Ti broad band was observed at 500–900 cm^{-1}, which indicates the interaction between TiO_2 nanoparticles and SGNs [36]. Additionally, another band around 442 cm^{-1} was observed, which indicates the formation of Ti–O–C bond during the synthesis process [37].

In order to understand the chemical composition and bonding environment for TiO_2/SGNs composites, XPS was conducted. Figs. 5a and b represent the core level C 1s and O 1s spectra for TiO_2/SGNs composites. The C1s spectrum could further be deconvoluted into four chemically shifted components and assigned to sp^2 C=C bond (284.7 eV), sp^3 C–C bond (285.2 eV), C–O single bond (286.7 eV) and C=O in O=C–O–C (288.9 eV), respectively [38]. The edge carbon atoms are bonded with C–O and C=O oxygen functional groups, among which the C=O is highly stable [39]. Some studies indicated the Ti–C bond formation in TiO_2 and carbon hybrid [40]. The Ti and C are bonded through the oxygen atom in order to form the possible C–O–Ti bonds. Further, the O 1s XPS spectra, as shown in Fig. 5b. The peak at 530.8 eV is due to the Ti–O–Ti, and the strong peak at 531.7 eV is believed to result from the Ti–O–C [41]. In the present case, the results indicate the hybrid formation in TiO_2/SGNs composites possibly through the Ti–O–C and Ti–O–Ti bonds. The core level Ti 2p XPS spectra of TiO_2/SGNs composites is provided in Fig. 5c. The peaks 458.1 eV and 463.9 eV are due to the Ti $2p_{3/2}$ and $2p_{1/2}$ orbital splitting of Ti 2p core level states in TiO_2 [41].

Fig. 6 shows DRS spectra of TiO_2, SGNs, TiO_2/SGNs composites, which are transformed into direct and indirect transition patterns. Fig. 6a indicates that the absorption edge of TiO_2/SGNs shift to the visible range in comparison with that of pure TiO_2, indicated that doped SGNs can make titanium dioxide respond to visible light [13]. The direct and indirect transition energy gaps were calculated from the absorption edges in Figs. 6b and c. The energy gap of anatase TiO_2 block was 3.2 eV, which was calculated by direct transition formula and in line with the actual value 3.2 eV. On the contrary, the band gap energy 2.70 eV of TiO_2 calculated by indirect transition is less than that of actual value from Fig. 6c. Moreover, the direct forbidden

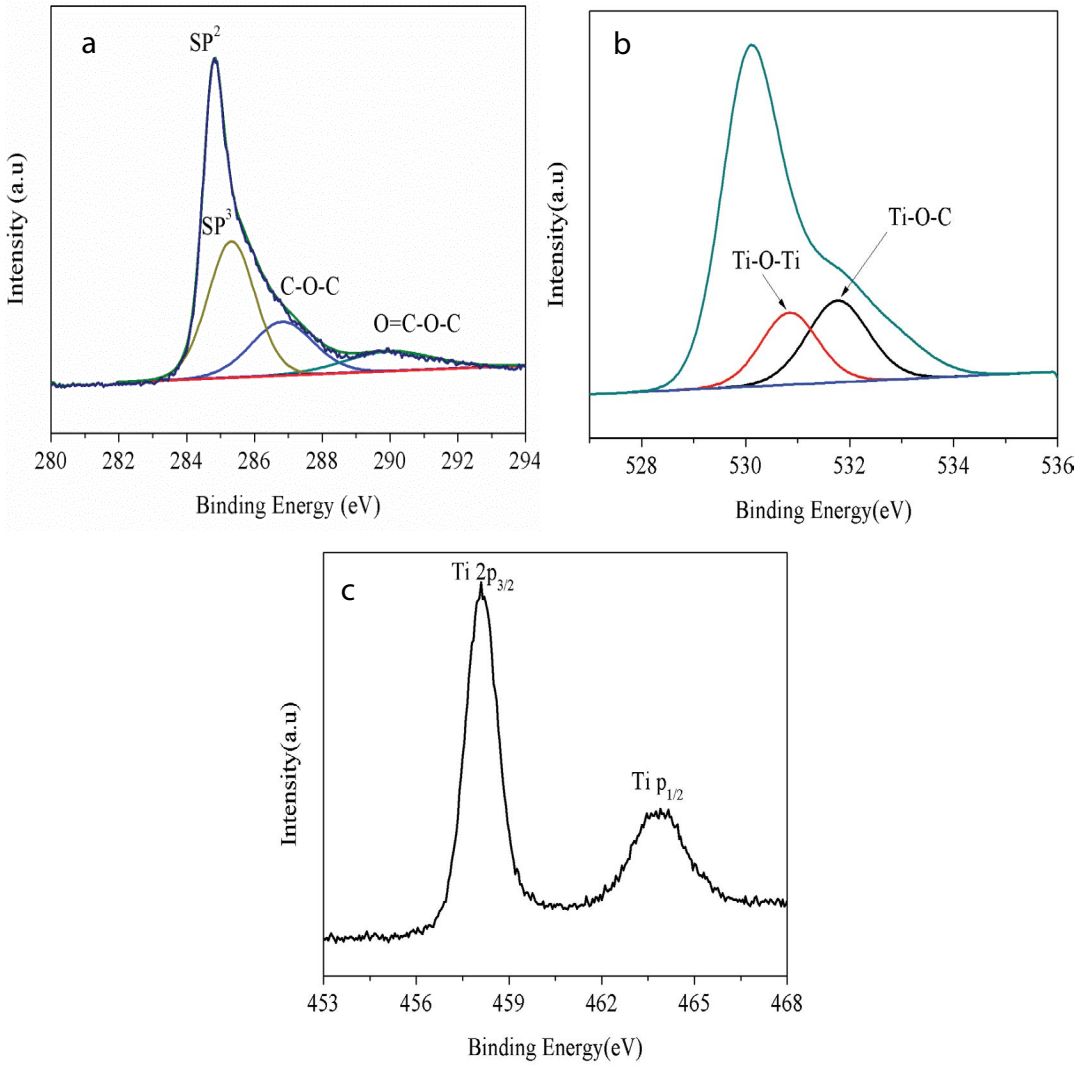

Fig. 5. Core level XPS spectra of TiO_2/SGNs composites (a) C1s spectra (b) O1s spectra and (c) Ti 2p, respectively.

band energy E_d for TiO_2/SGNs composites is 2.85 eV, lower than that of TiO_2 (3.2 eV). The results are consistent with that of Martins et al. [13] reported. The introduction of SGNs improved the adsorption of the pollutants onto the nanoparticles surface and increased separation of charge carriers, which effectively inhibited electron–hole pair and recombination, thus increased photocatalytic efficiency.

3.2. Photocatalytic degradation of MB

The degradation rate of MB increases with the increase of the amount of composite catalyst (Fig. 7a). When 100 mg TiO_2/SGNs was applied, the degradation rate of MB up to 97.07% was obtained; further increasing the dosage of TiO_2/SGNs to 140 mg, the degradation rate slightly decreased to 95.60%. It may be due to the light scattering of catalyst particles, which led to the decrease of light absorption ability, and the transmittance of light and the degradation rate [42]. Therefore, the optimum dosage of the composite of 100 mg was applied in the next studies.

Effect of pH on the degradation rate of MB by TiO_2/SGNs composites is shown in Fig. 7b. It was found that the alkaline environment is more favorable to the photocatalytic reaction than in acidic environment, and the highest degradation rate of (98.81%) was obtained at pH 11. The possible reason can be given that under acidic conditions, the surface of TiO_2/SGNs is positively charged, which is obviously not conducive to the catalysis of MB molecules by TiO_2. It is easier to degrade MB in alkaline conditions because the photocatalytic reactions were promoted mainly by the formation of the hydroxyl radicals (OH·). In addition, the surface of TiO_2/SGNs is negatively charged at the alkaline conditions, the photogenerated holes will also be transferred to the surface of the photocatalyst, increasing the active center and promoting photocatalytic degradation [43].

The effect of initial MB concentration and time is investigated in Fig. 7c. As shown, the degradation rate decreased with the increase of initial concentration of MB. The reason may be that with the increase of the concentration, the transmittance of the solution decreased and the photons showed

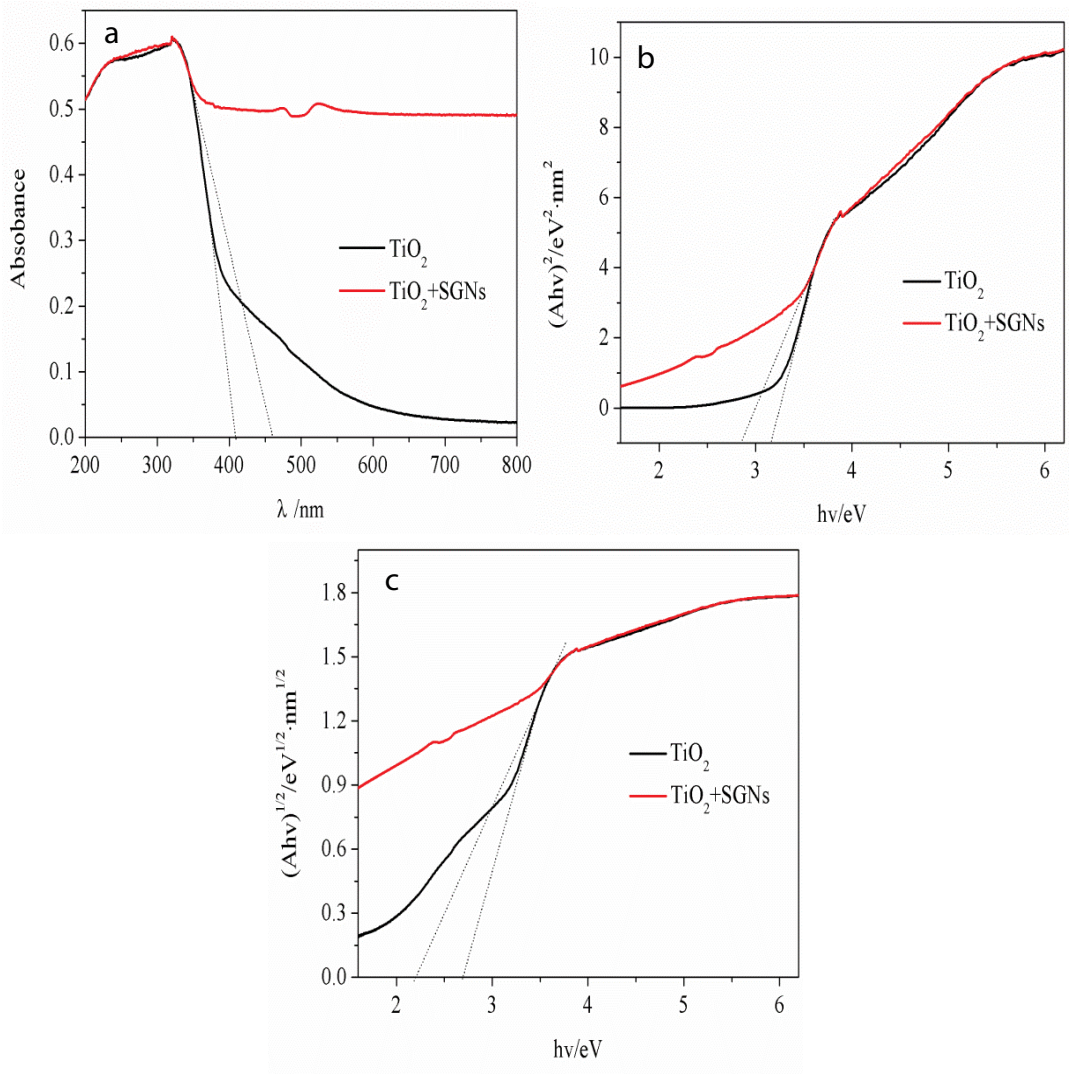

Fig. 6. DRS (a), direct gap (b) and indirect gap (c) transition patterns of TiO_2, SGNs, TiO_2/SGNs composites.

less contact with the dye molecules [44]. Whatever, the degradation rate of MB was positively correlated with the reaction time, and the degradation rate of MB was no longer increased after the reaction of 60 min. In the process of chemical reaction, the positive reaction and the inverse reaction were carried out simultaneously. After the reaction of 60 min, the chrominance removal rate did not change obviously because the reaction reached the chemical equilibrium. Therefore, the optimum reaction time is 60 min, which was more rapid than that of reference reported (MB concentration 10 mg L^{-1}, time 120 min) [45].

Stability is an important factor in evaluating the practical application of TiO_2/SGNs composites. In order to evaluate the stability of the prepared catalyst, under optimal conditions (TiO_2/SGNs dosage 100 mg, pH = 11, irradiated by ultraviolet light 60 min), the TiO_2/SGNs catalyst was recovered and reused to degrade MB under the same conditions. 98.81% MB degradation rate was obtained by TiO_2/SGNs for the first time, and there was no significant decrease in photocatalytic activity after consecutive four cycles of experiments. It suggested that TiO_2/SGNs has good stability and can be reused. Concerning the adsorption tests, large adsorption of MB dye onto the nanoparticles surface was observed within 60 min, for TiO_2/SGNs composites. For the TiO_2/SGNs sample, most of the dye was adsorbed onto the catalyst in the equilibration step which prevented the measurement of its photocatalytic activity. The enhanced removal of MB in photocatalysis is justified by the combination of photocatalysis of TiO_2 and adsorption of graphene. Raman spectrum TiO_2/SGNs after MB degradation is shown in Fig. 8. Overall, the high photocatalytic activity, excellent structural stability and good reproducibility make the synthesized photocatalyst as a qualified candidate for wastewater treatment.

3.3. Kinetics study

The kinetics for degradation of MB on dark reaction, SGNs, pure TiO_2 (MB concentration 20 mg L^{-1}) and TiO_2/SGNs composites (different initial concentration of MB

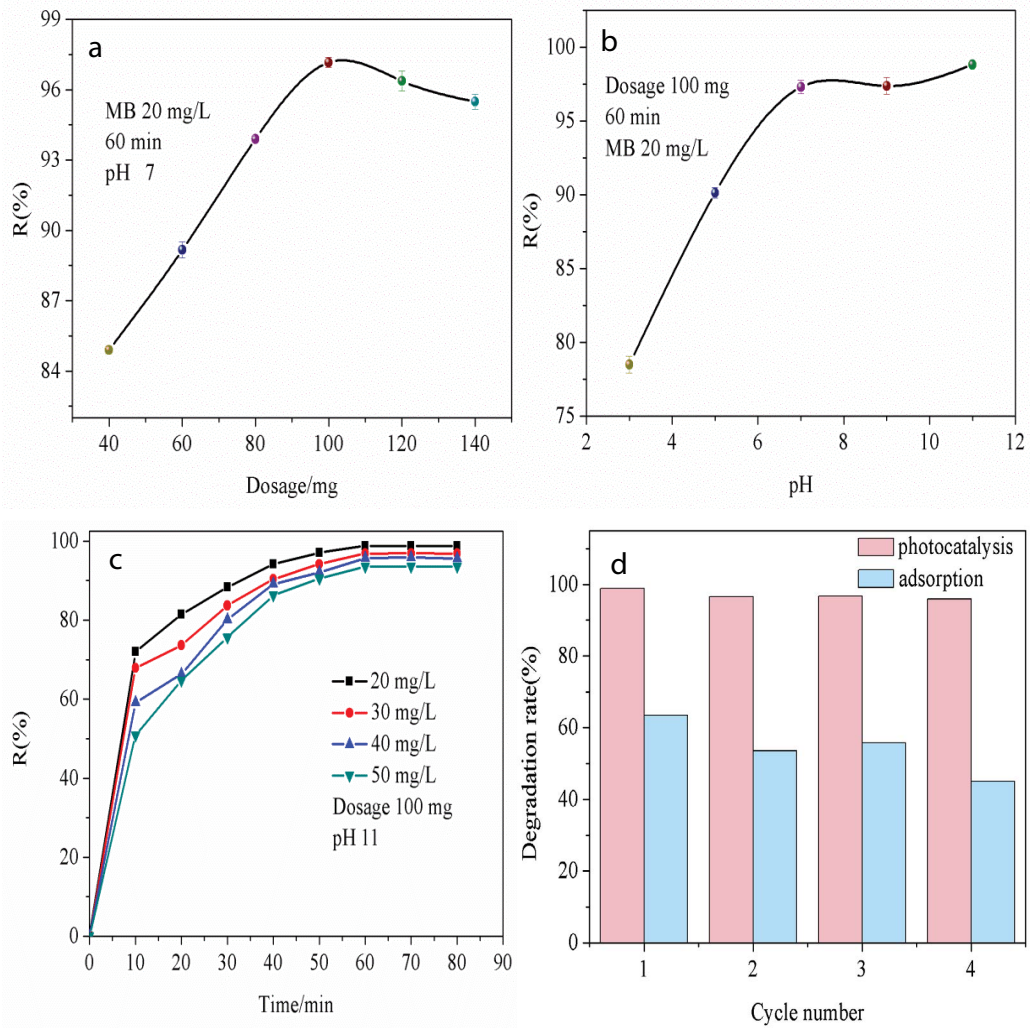

Fig. 7. Effect of parameters on the degradation rate of MB. (a) Dosage, (b) pH, (c) time, and (d) cyclic catalytic degradation rate of TiO_2/SGNs.

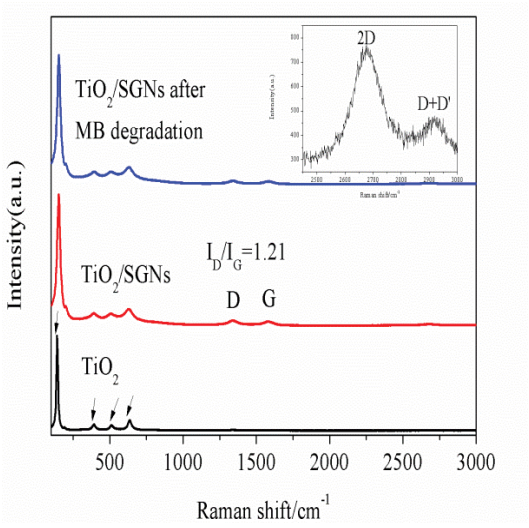

Fig. 8. Raman spectra of TiO_2 and TiO_2/SGNs before and after MB degradation.

20–50 mg L^{-1}) under UV irradiation is shown in Fig. 9. The apparent reaction rate (k), calculated from the slope of the exponential curve of the concentration plot in Fig. 9b. The results show that UV irradiation is more efficient than dark reaction, and TiO_2/SGNs composites are potentially more efficient than pure TiO_2 and SGNs (2 mg) with higher kinetics constant, indicating the combination of SGNs with TiO_2 enhanced greatly the photocatalytic activity of the TiO_2/SGNs composites.

With the increase of the initial concentration of MB, the apparent reaction rate constant decreases from 0.06292 to 0.04176 min^{-1}, indicating that the photocatalytic degradation rate is inversely proportional to the initial concentration of MB. At higher concentrations, the MB adsorption onto catalyst surface may reach saturation rapidly and slow down photocatalytic degradation [44], probably because electron transfer to the catalyst surface was intervened by adsorbed MB. Furthermore, MB and its intermediates could compete with each other for limited reactive sites on the catalyst surface, hence inhibiting the overall degradation of MB [46]. Compared with the literature reported [13,47,48], the

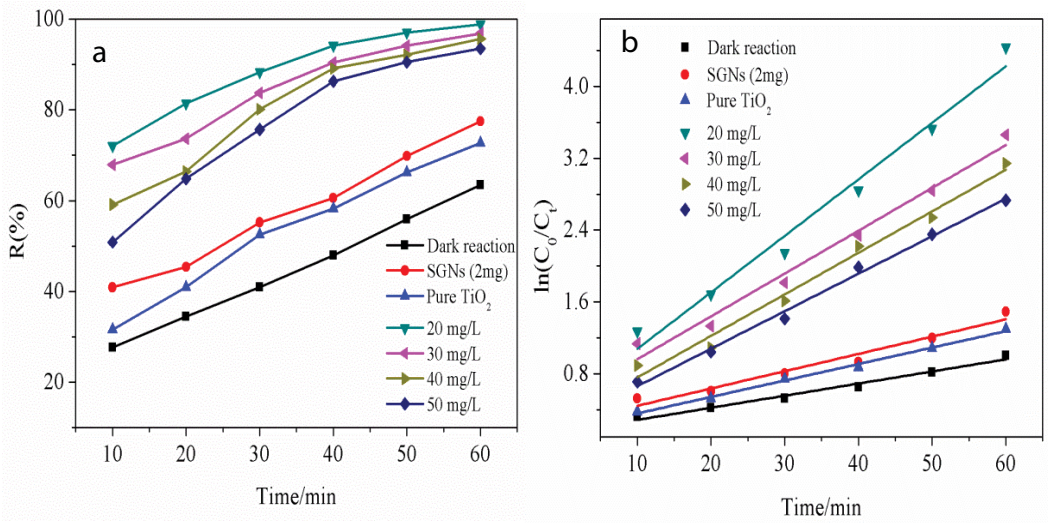

Fig. 9. (a) Degradation rate and (b) pseudo-first-order kinetics of MB under various conditions

moderate higher pseudo-first-order constants (k) were observed, indicating the excellent photocatalytic properties of the prepared TiO_2/SGNs composites catalyst.

4. Conclusion

A comprehensive work focused on TiO_2/SGNs prepared by hydrothermal method, and the experimental photocatalytic performance of these composites with different contents of SGNs was carried out. The results showed that TiO_2/SGNs composites are potentially more efficient than pure TiO_2, due to a large number of π–π conjugated double bonds on the surface of graphene and a large number of organic molecules can be enriched on the graphene plane. XRD and Raman spectra confirmed that the prepared TiO_2 is anatase type. FT-IR and XPS spectra demonstrated that the hybrid formation in TiO_2/SGNs composites possibly through the Ti–O–C and Ti–O–Ti bonds. Additionally, the direct forbidden band energy E_g (2.85 eV) of TiO_2/SGNs composites is lower than that of TiO_2 (3.2 eV). Photocatalytic experiments show that the optimum reaction conditions are TiO_2/SGNs dosage 100 mg, pH 11, irradiated by UV light for 60 min. Kinetic study showed that TiO_2/SGNs photocatalytic degradation of MB fitted well with pseudo-first-order reaction, and the apparent reaction rate (k) decreases with increasing MB concentration. Thus, the photocatalytic experiments showed that the TiO_2/SGNs composites are efficient catalytic agents for the degradation of the MB.

References

[1] N. Bensalah, M.A. Quiroz Alfaro, C.A. Martínez-Huitle, Electrochemical treatment of synthetic wastewaters containing Alphazurine A dye, Chem. Eng. J., 149 (2009) 348–352.
[2] M. Doğan, Y. Özdemir, M. Alkan, Adsorption kinetics and mechanism of cationic methyl violet and methylene blue dyes onto sepiolite, Dyes Pigm., 75 (2007) 701–713.
[3] K. Nakata, A. Fujishima, TiO_2 photocatalysis: design and applications, J. Photochem. Photobiol., C, 13 (2012) 169–189.
[4] D. Spasiano, R. Marotta, S. Malato, P. Fernandez-Ibañez, I. Di Somma, Solar photocatalysis: materials, reactors, some commercial, and pre-industrialized applications. A comprehensive approach, Appl. Catal., B, 170–171 (2015) 90–123.
[5] K. Hashimoto, H. Irie, A. Fujishima, TiO_2 photocatalysis: a historical overview and future prospects, Jpn. J. Appl. Phys., Part 1, 44 (2005) 8269–8285.
[6] S.N. Frank, A.J. Bard, Heterogeneous photocatalytic oxidation of cyanide and sulfite in aqueous solutions at titanium dioxide powder, J. Am. Chem. Soc., 8 (1977) 303–304.
[7] P.M. Martins, V. Gomez, A.C. Lopes, C.J. Tavares, G. Botelho, S. Irusta, Improving photocatalytic performance and recyclability by development of Er-doped and Er/Pr-codoped TiO_2/poly(vinylidene difluoride)–trifluoroethylene composite membranes, J. Phys. Chem. C, 118 (2014) 27944–27953.
[8] N.A. Almeida, P.M. Martins, S. Teixeira, J.A.L. da Silva, V. Sencadas, K. Kühn, G. Cuniberti, S. Lanceros-Mendez, P.A.A.P. Marques, TiO_2/graphene oxide immobilized in P(VDF-TrFE) electrospun membranes with enhanced visible-light-induced photocatalytic performance, J. Mater. Sci., 51 (2016) 6974–6986.
[9] E.A. Kozlova, A.V. Vorontsov, Noble metal and sulfuric acid modified TiO_2 photocatalysts: mineralization of organo-phosphorous compounds, Appl. Catal., B, 63 (2006) 114–123.
[10] R. Marschall, L. Wang, Non-metal doping of transition metal oxides for visible-light photocatalysis, Catal. Today, 225 (2014) 111–135.
[11] T. Lavanya, M. Dutta, S. Ramaprabhu, K. Satheesh, Superior photocatalytic performance of graphene wrapped anatase/rutile mixed phase TiO_2 nanofibers synthesized by a simple and facile route, J. Environ. Chem. Eng., 5 (2017) 494–503.
[12] P.C. Yao, S.H. Zhong, Z.R. Shen, TiO_2/halloysite composites codoped with carbon and nitrogen from melamine and their enhanced solar-light-driven photocatalytic performance, Int. J. Photoenergy, 2015 (2015) 605690.
[13] P.M. Martins, C.G. Ferreira, A.R. Silva, B. Magalhães, M.M. Alves, L. Pereira, P.A.A.P. Marques, M. Melle-Franco, S. Lanceros-Méndez, TiO_2/graphene and TiO_2/graphene oxide nanocomposites for photocatalytic applications: a computer modeling and experimental study, Composites Part B, 145 (2018) 39–46.
[14] Q. Huang, S. Tian, D. Zeng, X. Wang, W. Song, Y. Li, W. Xiao, C. Xie, Enhanced photocatalytic activity of chemically bonded TiO_2/graphene composites based on the effective interfacial charge transfer through the C–Ti bond, ACS Catal., 7 (2013) 1477–1485.
[15] Y. Chen, J. Wang, W. Li, Research progress of new titanium dioxide based photocatalytic materials, J. Mater. Eng., 44 (2016) 103–113.

[16] J. Liu, L. Wang, J. Tang, J. Ma, Photocatalytic degradation of commercially sourced naphthenic acids by TiO_2-graphene composite nanomaterial, Chemosphere, 149 (2016) 328–335.
[17] H. Zhang, X. Lv, Y. Li, Y. Wang, J. Li, P25-graphene composite as a high performance photocatalyst, ACS Nano, 4 (2009) 380–386.
[18] P. Calza, C. Hadjicostas, V.A. Sakkas, M. Sarro, C. Minero, C. Medana, T.A. Albanis, Photocatalytic transformation of the antipsychotic drug risperidone in aqueous media on reduced graphene oxide—TiO_2 composites, Appl. Catal., B, 183 (2016) 96–106.
[19] Z. Zhang, F. Xiao, Y. Guo, S. Wang, Y. Liu, One-pot self-assembled three-dimensional TiO_2-graphene hydrogel with improved adsorption capacities and photocatalytic and electrochemical activities, ACS Appl. Mater. Interfaces, 5 (2013) 2227–2233.
[20] B. Qiu, M. Xing, J. Zhang, Mesoporous TiO_2 nanocrystals grown in situ on graphene aerogels for high photocatalysis and lithium-ion batteries, J. Am. Chem. Soc., 136 (2014) 5852–5855.
[21] R.M. Jugade, S. Sharma, S. Gokhale, CVD synthesis of graphene nanoplates on MgO support, Mater. Sci. Poland, 32 (2014) 243–246.
[22] G. Ning, Z. Fan, G. Wang, J. Gao, W. Qian, F. Wei, Gram-scale synthesis of nanomesh graphene with high surface area and its application in supercapacitor electrodes, Chem. Commun., 47 (2011) 5976–5978.
[23] E. Mooser, W.B. Pearson, A.F. Gibson, Progress in Semiconductors, John Wiley & Sons, 5 (1960) 53–60.
[24] R.K. Madhusudan, S.V. Manorama, A.R. Reddy, Bandgap studies on anatase titanium dioxide nanoparticles, Mater. Chem. Phys., 78 (2002) 239–245.
[25] M.R. Hoffmann, S.T. Martin, W. Choi, D.W. Bahnemann, Environmental applications of semiconductor photocatalysis, Chem. Rev., 95 (1995) 69–96.
[26] S.G. Kumar, L.G. Devi, Review on modified TiO_2 photocatalysis under UV/visible light: selected results and related mechanisms on interfacial charge carrier transfer dynamics, J. Phys. Chem. A, 115 (2011) 13211–13241.
[27] L.M. Pastrana-Martínez, S. Morales-Torres, V. Likodimos, J.L. Figueiredo, J.L. Faria, P. Falaras, A.M.T. Silva, Advanced nanostructured photocatalysts based on reduced graphene oxide–TiO_2 composites for degradation of diphenhydramine pharmaceutical and methyl orange dye, Appl. Catal., B, 123–124 (2012) 241–256.
[28] F. Dufour, S. Pigeot-Remy, S. Durupthy, S. Cassaignon, V. Ruaux, S. Torelli, L. Mariey, F. Maugé, C. Chanéac, Morphological control of TiO_2 anatase nanoparticles: what is the good surface property to obtain efficient photocatalysts?, Appl. Catal., B, 174–175 (2015) 350–360.
[29] T.N. Blanton, D. Majumdar, Characterization of X-ray irradiated graphene oxide coatings using X-ray diffraction, X-ray photoelectron spectroscopy, and atomic force microscopy, Powder Diffr., 28 (2013) 68–71.
[30] H. Feng, R. Cheng, X. Zhao, X. Duan, J. Li, A low-temperature method to produce highly reduced graphene oxide, Nat. Commun., 4 (2013) 1539–1546.
[31] T. Lavanya, K. Satheesh, M. Dutta, N.V. Jaya, N. Fukata, Superior photocatalytic performance of reduced graphene oxide wrapped electrospun anatase mesoporous TiO_2 nanofiber, J. Alloys Compd., 615 (2014) 643–650.
[32] J. Yang, S. Mei, J.M.F. Ferreira, Hydrothermal synthesis of nanosized titania powders: influence of peptization and peptizing agents on the crystalline phases and phase transitions, J. Am. Ceram. Soc., 83 (2000) 1361–1368.
[33] Y. Iida, S. Ozaki, Grain growth and phase transformation of titanium oxide during calcination, J. Am. Ceram. Soc., 44 (2010) 120–127.
[34] F. Tuinstra, J.L. Koenig, Raman spectrum of graphite, J. Chem. Phys., 53 (1970) 1126–1130.
[35] J. Maultzsch, S. Reich, C. Thomsen, Double-resonant Raman scattering in graphite: interference effects, selection rules, and phonon dispersion, Phys. Rev. B: Condens. Matter, 70 (2004) 2806–2810.
[36] T. Lavanya, M. Dutta, K. Satheesh, Graphene wrapped porous tubular rutile TiO_2 nanofibers with superior interfacial contact for highly efficient photocatalytic performance for water treatment, Sep. Purif. Technol., 168 (2016) 284–293.
[37] H.K. Yu, Effective reduction of copper surface for clean graphene growth, J. Electrochem. Soc., 12 (2015) 277–281.
[38] G. Rajender, P.K. Giri, Formation mechanism of graphene quantum dots and their edge state conversion probed by photoluminescence and Raman spectroscopy, J. Mater. Chem. C, 4 (2016) 10852–10865.
[39] S. Umrao, S. Abraham, F. Theil, S. Pandey, V. Ciobota, P.K. Shukla, C.J. Rupp, S. Chakraborty, R. Ahuja, J. Popp, B. Dietzek, A. Srivastava, A possible mechanism for the emergence of an additional band gap due to a Ti–O–C bond in the TiO_2–graphene hybrid system for enhanced photodegradation of methylene blue under visible light, RSC Adv., 4 (2014) 59890–59901.
[40] B. Santara, P.K. Giri, K. Imakita, M. Fujii, Evidence of oxygen vacancy induced room temperature ferromagnetism in solvothermally synthesized undoped TiO_2 nanoribbons, Nanoscale, 5 (2013) 5476–5488.
[41] J.S. Lee, K.H. You, C.B. Park, Highly photoactive, low bandgap TiO_2 nanoparticles wrapped by graphene, Adv. Mater., 24 (2012) 1133–1133.
[42] Y.B. Zhang, B. Chen, Factors affecting degradation of Methyl Violet catalyzed by visible light of titanium dioxide, Appl. Chem. Ind., 40 (2011) 814–816.
[43] H.B. Hadjltaief, P. Da Costa, M.E. Galvez, M.B. Zina, Influence of operational parameters in the heterogeneous photo-Fenton discoloration of wastewaters in the presence of an iron-pillared clay, Ind. Eng. Chem. Res., 52 (2013) 16656–16665.
[44] S.K. Kansal, M. Singh, D. Sud, Studies on photodegradation of two commercial dyes in aqueous phase using different photocatalysts, J. Hazard. Mater., 141 (2007) 581–590.
[45] N. Zhang, B. Li, S. Li, S. Yang. Graphene-supported mesoporous titania nanosheets for efficient photodegradation, J. Colloid Interface Sci., 505 (2017) 711–718.
[46] B. Zhou, X. Zhao, H. Liu, J. Qu, C.P. Huang, Visible-light sensitive cobalt-doped $BiVO_4$ (Co-$BiVO_4$) photocatalytic composites for the degradation of methylene blue dye in dilute aqueous solutions, Appl. Catal., B, 99 (2010) 214–221.
[47] M. Minella, F. Sordello, C. Minero, Photocatalytic process in TiO_2/graphene hybrid materials. Evidence of charge separation by electron transfer from reduced graphene oxide to TiO_2, Catal. Today, 281 (2017) 29–37.
[48] J. Suave, S.M. Amorim, R.F.P.M. Moreira, TiO_2-graphene nanocomposite supported on floating autoclaved cellular concrete for photocatalytic removal of organic compounds, J. Environ. Chem. Eng., 5 (2017) 3215–3223.